

## High Rydberg Atoms: Newcomers to the Atomic Physics Scene

The availability of new technology has paved the way for studies of these huge and fragile atoms.

Ronald F. Stebbings

Normal atoms are so small that a billion of them placed in a row would stretch only a few inches. However, if they are perturbed in certain ways their size may be vastly increased. They may, in fact, attain the dimensions of small biological molecules and become as large compared to normal atoms as such atoms are compared to their nuclei. The consequences of such a change are numerous and fascinating. It becomes necessary, for example, to consider the limiting size of an aperture through which such atoms can pass. It is amusing to recognize that because of their great size, the probability of finding other atoms "inside" them becomes appreciable even at quite low pressures.

To gain an understanding of these curiosities one may begin by noting that the allowed energy states of the hydrogen atom are given with good accuracy by the expression

$$E_n = - \frac{13.6}{n^2} \text{ ev}$$

where  $n$ , the principal quantum number, takes positive integral values. It is customary to represent these states by the term diagram shown in Fig. 1, where their energies are given in electron volts relative to the ground state ( $n = 1$ ) and in wave numbers, in units of reciprocal centimeters where  $1 \text{ ev} = 8065.7 \text{ cm}^{-1}$ , relative to the ionization limit ( $n = \infty$ ). Transitions between these states give

rise to groups of lines such as those of the well-known Lyman and Balmer series. Until quite recently interest was focused primarily on the first few excited states, with  $n$  up to about 5. However, this situation is changing rapidly, and a number of experimental and theoretical investigations of much more highly excited atoms ( $n$  up to  $\sim 80$ ) are currently under way.

For these "high Rydberg" states the Bohr model of the hydrogen atom, in which an electron moves in orbit around a proton, may be taken seriously. A few classical properties of the hydrogen atom are given in Table 1 for arbitrary  $n$  and for  $n = 1$  and 100. It is immediately evident that highly excited atoms have some quite astonishing characteristics and bear little resemblance to unexcited atoms. An example is their enormous size. Their geometric cross section scales as  $n^4$  and for  $n = 100$  is  $10^8$  times that for ground state atoms. For highly excited atoms the electron is only very weakly bound to the proton. The energy required to ionize hydrogen atoms with  $n = 100$  is, for example, only 1.36 meV, and such atoms are therefore extremely fragile. Furthermore, the energy separation between adjacent excited states varies as  $n^{-3}$ . For  $n = 100$  this separation is  $2.7 \times 10^{-5} \text{ ev}$  or  $0.21 \text{ cm}^{-1}$  and excitation of atoms to a single highly excited state therefore necessitates a technique with extremely high energy resolution.

Many of the present studies concern

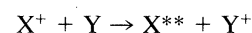
highly excited states of atoms other than hydrogen. However, for sufficiently large values of  $n$ , a high Rydberg atom of any species consists of a single excited electron far removed from its ionic core. If the electron has sufficient angular momentum that it does not appreciably penetrate the core, the remaining electrons will effectively screen from it all but one nuclear charge, so that it moves essentially in a Coulomb field of unit charge. Such atoms thus very closely resemble hydrogen.

The motivation for studying such atoms is quite varied. Apart from their intrinsic interest, they are pertinent to such diverse fields as laser development, laser isotope separation, energy deposition in gases, plasma diagnostics, and radio astronomy, to name a few.

### Production of High Rydberg Atoms

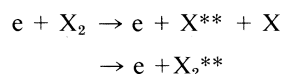
To date, production of high Rydberg atoms has been accomplished by three techniques.

#### 1) Charge transfer between $X^+$ and $Y$



where  $X^{**}$  is a high Rydberg atom.

#### 2) Electron impact excitation



where  $e$  is an electron.

#### 3) Photon impact



where  $h\nu$  is a photon and  $l$  is the azimuthal quantum number.

High Rydberg atoms produced in charge transfer collisions of fast ions during passage through a gaseous target have been studied by several investigators. Riviere and Sweetman (1) observed the production of hydrogen atoms in states with  $n = 9$  to 23 and II' in *et al.* (2) investigated the production of helium atoms in states with  $n = 9$  to 17. Bay-

The author is professor of space physics and astronomy and of physics at Rice University, Houston, Texas 77001.

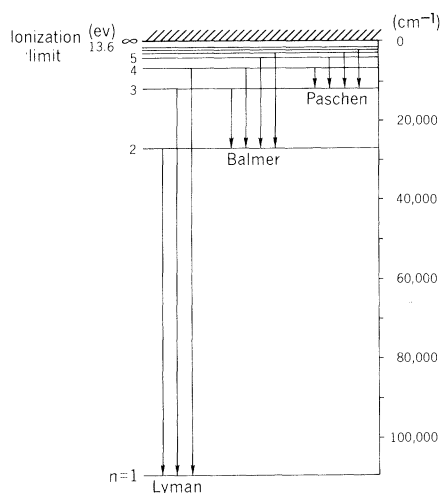


Fig. 1. Partial term diagram for hydrogen.

field and Koch (3) have studied mixtures of highly excited hydrogen atoms within the range  $44 \leq n \leq 69$  and observed that at kilovolt energies the cross section for production of high Rydberg atoms scales as  $n^{-3}$ .

The technique of electron impact excitation has been used quite widely. Cermak and Herman (4), Hotop and Niehaus (5), Kupriyanov (6), and Shibata *et al.* (7) have all used this method to produce beams of high Rydberg atoms with an unknown mixture of  $n$  in the range  $n = 20$  to 40. Recently Freund and his colleagues (8) have examined the high Rydberg particles produced by excitation of various atoms and molecules. Representative of these measurements are those for  $H_2$  (9, 10) in which a beam of electrons with energy in the range  $20 \text{ eV} \leq E \leq 100 \text{ eV}$  and an energy spread  $\Delta E \sim 0.3 \text{ eV}$  was crossed with an  $H_2$  beam. High Rydberg species emerging from the collision region at right angles to the electron and hydrogen beams were detected at a distance of about 20 cm from the interaction region. Time-of-flight studies led to the identification of five distinct high Rydberg components, for each of which an excitation mechanism has been proposed. Donohue *et al.* (10) observed states with  $n$  between 14 and 80. The population peaks between  $n = 17$  and  $n = 40$ , depending on the flight time from the interaction

region to the detector, decreasing as  $n^{-3}$  at large  $n$  and decreasing at small  $n$  due to radiative decay. Relative and absolute excitation cross sections were determined.

The main limitation of both these experimental techniques is that in neither case can a beam of atoms in a single high Rydberg state be produced. The energy resolution needed to achieve this is, in fact, attainable at the present time only by optical means. Much of the pioneering work in this was carried out by Chupka (11) using the highly dispersed light from a continuum source. In this manner highly excited rare gas atoms with  $n$  up to about 25 were excited directly from the ground state and many of their properties have been studied.

It is the growing availability of tunable lasers, however, that has provided the impetus for the current surge of activity in this field. At the present time tunable lasers are, by and large, restricted to wavelengths longer than  $2300 \text{ \AA}$  (12), which corresponds to photon energies a little above 5 eV. Because of this limitation the highly excited states of most atoms are not directly accessible in a single-photon absorption from the ground state with a laser, and various excitation schemes have been devised to circumvent this problem.

In one such approach Stebbings *et al.* (13) produced high Rydberg atoms of xenon in a two-step process incorporating both electron and photon excitation, as illustrated in Fig. 2. In these experiments a beam of ground state xenon atoms was excited with an electron beam, and metastable atoms in the  $^3P_0$  state were produced. These atoms were then irradiated with the output of a pulsed tunable dye laser, which resulted in the population of highly excited  $p$  and  $f$  states with  $n$  in the range 8 to 40. The identity of these excited levels was established unambiguously by a comparison of their term values with those obtained by an extrapolation from the previously tabulated lower members of these series. The excitation of  $f$  states is an apparent violation of the selection rule  $\Delta l = \pm 1$ . In reality, however, it is an indication that one or both of the levels involved in

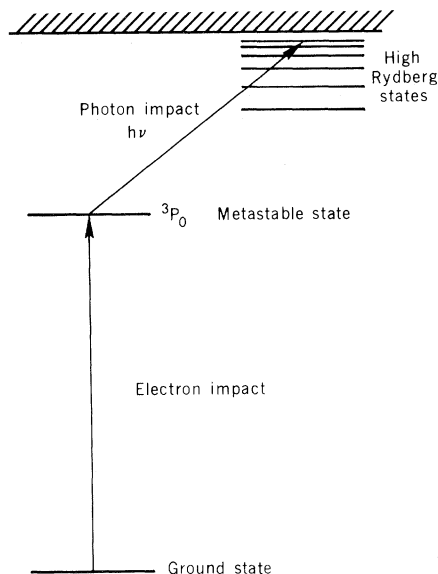


Fig. 2. Production of high Rydberg atoms in a two-step process incorporating both electron and photon excitation.

the transition are better described by superposition of configurations.

High Rydberg states of sodium have been populated by using the process, illustrated in Fig. 3, in which stepwise excitation to high-lying  $s$  and  $d$  states is accomplished by two pulsed dye lasers excited by the same  $N_2$  laser. One dye laser is used to saturate the  $D_1$  line at  $5890 \text{ \AA}$ , creating a large population in the  $3p$  state, while the second laser excites transitions from this state to the high-lying  $s$  or  $d$  states. In this manner states with principal quantum numbers between 5 and 40 have been individually populated (14, 15).

The identity of the excited levels was determined as  $s$  or  $d$  by Ducas *et al.* (15) with a refinement of this technique, which takes advantage of the fact that the selection rules for stepwise two-photon processes are influenced by nuclear coupling in the intermediate state. The electron-nucleus hyperfine interaction mixes states of different quantum numbers  $m_J$  and  $m_I$  (where  $\hbar J$  and  $\hbar I$  are the electron and nuclear angular momenta) to create a state of total angular momentum  $\hbar F$ . This tends to scramble together states of all possible values of  $m_J$  and  $m_I$  that satisfy  $m_J + m_I = m_F$ . As a consequence, continuous-wave (CW) absorption of two photons circularly polarized in the same sense gives rise both to  $s \rightarrow p \rightarrow s$  and  $s \rightarrow p \rightarrow d$  transitions. In contrast, if two such photons are absorbed successively in a short time compared to the hyperfine period of the intermediate state, the electron does not have time to precess about the nucleus to a new spatial orientation before it absorbs

Table 1. Properties of the hydrogen atom.

Property	$n = 1$	Arbitrary $n$	$n = 100$
Radius of Bohr orbit (cm)	$a_0 = 5.3 \times 10^{-9}$	$n^2 a_0$	$5.3 \times 10^{-5}$
Geometric cross section (cm <sup>2</sup> )	$\pi a_0^2 = 8.8 \times 10^{-17}$	$n^4 \pi a_0^2$	$8.8 \times 10^{-9}$
Binding energy, $ E_n $ (eV)	$R_H = 13.6$	$R_H/n^2$	$1.36 \times 10^{-3}$
Root-mean-square velocity of electron (cm/sec)	$v_1 = 2.2 \times 10^8$	$v_1/n$	$2.2 \times 10^6$
Separation of adjacent $n$ levels (eV)		$2R_H/n^3$	$2.7 \times 10^{-5}$

the second photon. In this case the electric dipole selection rules are the same as those for an atom with no nuclear spin, and  $s \rightarrow p \rightarrow s$  transitions are thus forbidden. It was observed that when the lasers were circularly polarized in the same sense the population of the  $s$  levels was a sensitive function of the delay between the pulses. Thus, when the delay was less than  $\sim 3$  nsec—that is, short compared to the hyperfine period—the transition rate to the  $s$  state was radically suppressed, whereas the rate to the  $d$  state was essentially unchanged. When the delay of the second pulse was increased to 8 nsec the  $s$  state transition rate was affected far less by circular polarization of the lasers.

It is evident that the optical excitation technique as described here leads to the population of states with low angular momentum only. States with high angular momentum are inaccessible because of the selection rule  $\Delta l = \pm 1$ , which in a two-photon excitation process restricts the total change in  $l$  to 0 or 2. Thus, for sodium with a  $3s$  ground state the highly excited states are  $s$  and  $d$ . However, Littman *et al.* (16) have developed a technique that circumvents this restriction and results in the population of states with high angular momentum. The essential feature of this method is that the excitation takes place in an electric field. The effect of this field is to polarize the atom and displace the  $l \geq 2$  terms, which were originally degenerate by an amount given in atomic units (17) by

$$\Delta E = 3n(n_1 - n_2)\mathcal{E}/2$$

Here  $\mathcal{E}$  is the electric field and  $n_1$  and  $n_2$  are two new quantum numbers, which satisfy  $n_1 + n_2 + |m| + 1 = n$ , where  $m$  is the magnetic quantum number. The difference  $n_1 - n_2$  is often called the electric quantum number. This is the first-order Stark effect. Now the important thing is that there is no selection rule with respect to the quantum numbers  $n_1$  and  $n_2$ , although transitions that involve a change in the sign of  $n_1 - n_2$  are generally weak. Thus in the presence of an electric field transitions to all the Stark components may be effected. However each of these Stark states connects adiabatically to a single angular momentum state at zero electric field. Thus by exciting the atom in the presence of an electric field, in which the first-order Stark structure is resolved, and then reducing the field to zero, states with any desired value of  $l$  can be populated.

A production technique based on an entirely different concept has been described by Koch *et al.* (18). In this experi-

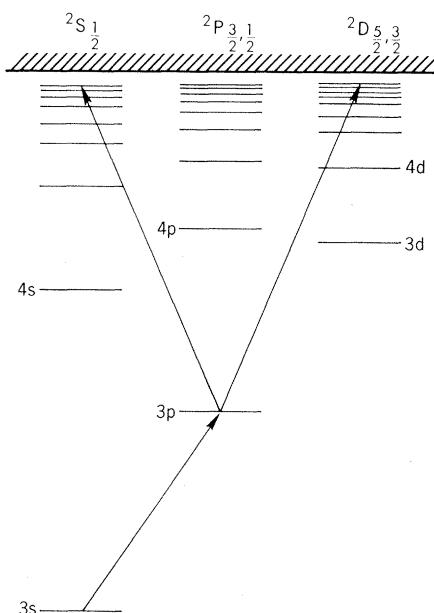


Fig. 3. Stepwise photoexcitation of sodium high Rydberg atoms.

ment a beam of fast H( $2s$ ) metastable atoms is produced by electron transfer collisions of a proton beam passing through an H<sub>2</sub> gas target. A fixed-frequency CW argon ion laser beam at 363.789 nm is directed colinear with the atomic beam and transitions to states with  $40 \leq n \leq 65$  are "Doppler tuned" into resonance by varying the energy of the atom beam. Portions of the resulting spectrum are shown in Fig. 4 and the different peaks are seen to be well resolved. This technique may be extended by the use of a CO<sub>2</sub> laser to "Doppler fine tune" with each of the many available laser lines near 10  $\mu\text{m}$  (18). For this work the initial state pumped by the laser light would be  $n = 10$ , which would be produced by electron transfer.

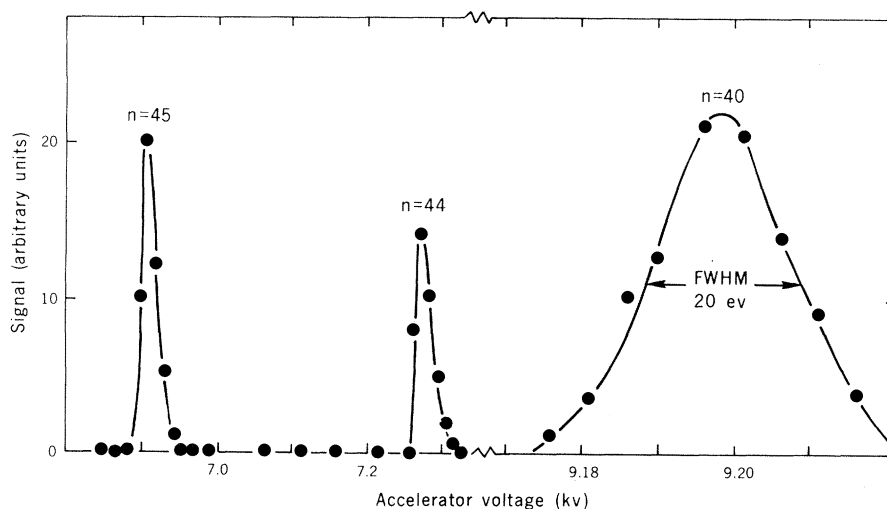


Fig. 4. Portions of the Doppler-tuned laser excitation spectrum  $\text{H}(2s) + h\nu \rightarrow \text{H}(nl)$ ; FWHM = full width at half maximum.

## Detection of High Rydberg Atoms

High Rydberg atoms may be detected in several ways. The radiation they emit spontaneously may be detected, as may the charged particles—positive ions and electrons—that result from their impact on a surface. The most versatile scheme used to date, however, is one based on field ionization, which may be understood with reference to Fig. 5.

The potential energy,  $-e^2/r$ , of the electron in a hydrogen-like atom in the absence of an external electric field is shown on the left in Fig. 5. The superposition of the potential  $-e\mathcal{E}z$  (sloping line) of an external field,  $\mathcal{E}$ , along the  $z$  direction not only perturbs the atomic energy levels (Stark effect) but also causes a potential maximum to appear on the "down-field" side of the atom. Quantum mechanics shows that the excited electron has a finite probability of tunneling through this potential barrier to the outside. At sufficiently high electric fields the barrier disappears and the electron moves freely away from the proton. The penetrability of this barrier was first calculated by Lanczos (19), whose work was later extended by Bailey *et al.* (20) to include all states up to  $n = 25$  and their substates.

It is interesting to note that in a given applied field the ionization probability for atoms occupying levels displaced upward by the applied field (that is, with  $n_1 - n_2$  positive in the expression for  $\Delta E$ ) is an order of magnitude lower than that for levels displaced downward. This, at first glance, is contrary to expectation, since for the levels displaced upward the barrier to ionization is smaller and hence more penetrable. However this effect is more than offset by the fact

that for levels displaced upward the electron spends most of its time on the side of the atom away from the barrier, while for those displaced downward the reverse is true. Field ionization has been observed experimentally in a number of laboratories. In the work of Stebbings *et al.* (13) Xe( $^3P_0$ ) metastable atoms in a field-free region were excited with a laser pulse of  $\sim 5$  nsec to the Rydberg state of interest. Then, after a 0.5- $\mu$ sec delay, an electric field  $\mathcal{E}$  was applied and the ions created were counted with a particle detector. Measurements were made of the ion production as a function of the strength of the applied field; the results for Xe(28f) are shown in Fig. 6. For fields less than about 600 volt/cm few ions were created because the barrier was essentially impenetrable. With a small increment in the field strength, however, a sharp increase in the ion signal was observed, after which further increases in the field strength led to no increase in ion production. This plateau signifies that all high Rydberg atoms present were ionized by the field and that the number of ions detected was equal to the number of high Rydberg atoms originally present. This detection scheme is therefore absolute, and furthermore the critical field  $\mathcal{E}_c$  depends strongly on the state of excitation of the atom. Thus, in an environment containing atoms in a variety of high Rydberg states, the application of a field of increasing strength will result in an increment in the ionization signal as the critical field for each state is reached.

A variation of this technique has been described by Koch *et al.* (18), who used microwaves rather than d-c fields to induce ionization. Plots of ionization rate against microwave power for various excited states show similar onset and saturation behavior.

### Studies with High Rydberg Atoms

Despite the relative infancy of this field, a variety of experimental studies have already been completed. Much of the initial work has been concentrated on the fundamental properties of high Rydberg atoms, such as their natural lifetimes. Studies of this type for xenon (13) with  $25 \leq n \leq 40$  and for sodium (14) with  $7 \leq n \leq 13$  demonstrate that the lifetimes increase approximately as  $n^3$ , in agreement with hydrogenic theory. For xenon additional studies showed that the lifetimes depend sensitively on the electric field to which the atoms are exposed. For example, the lifetime of the 28f state changes from 8 to 24  $\mu$ sec when the field is increased from 0 to 25 volt/cm. This effect is presumably due to Stark-induced mixing of the substates of the  $n$  level since, according to hydrogenic theory, the lifetime of an  $n$  level averaged over all substates should increase as  $\sim n^{4.5}$ .

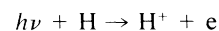
The study of fine-structure intervals (21, 22) in highly excited states has been discussed by MacAdam and Wing (21). In some of these states the structure is inverted (that is, states with higher values of the total angular momentum, described by the quantum number  $j$ , lie lower), while in others the structure is normal, as given by the ordinary theory of one-electron atoms. Recently Fabre *et al.* (23) measured the signs and absolute values of the fine-structure intervals for sodium  $nd$  states ( $9 \leq n \leq 16$ ) prepared by stepwise excitation with two pulsed lasers. Because of the pulsed character of this excitation the  $d$  states are prepared in a coherent superposition of  $j = 3/2$  and  $j = 5/2$  fine-structure components. The subsequent fluorescence resulting from decay back to the  $3p$  state exhibits quantum beats at the Bohr fre-

quency corresponding to the separation of these two components. Measurement of this frequency thus provides the absolute value of the fine-structure constant of this level.

Related studies have been carried out by Gallagher *et al.* (24), who report resonance measurements of the  $d-f$  splitting in highly excited states of sodium. They used stepwise photoexcitation (Fig. 3) to excite  $nd$  atoms, which were then irradiated with microwaves, inducing  $d \rightarrow f$  transitions. Decay from these  $f$  states to  $3d$  provides fluorescence in the range 8000 to 8500 Å, which is used to monitor the  $d-f$  resonances. These observations provide precise values of the  $d$  and  $f$  quantum defects as well as the  $d$  and  $f$  fine-structure splittings.

Much of the earlier theoretical interest (25) in high Rydberg atoms was sparked by the observations with radio telescopes of the interstellar radio recombination lines. The intensity of this radiation is observed as a function of wavelength, angle, and time, and provides information on the physical conditions, origin, and chemical composition of the emitting region.

Several processes lead to the emission of this radiation. Photoionization of ground state atoms



followed by recombination



may lead to highly excited atoms  $\text{H}_n$ . Spontaneous emission by these excited atoms is usually negligible, and the observed radiation is almost entirely a consequence of the stimulated emission



due to background continuum radiation, which arises predominantly from the process  $\text{Y}^+ + e \rightarrow \text{Y}^+ + e + h\nu$ , where  $\text{Y}^+ = \text{H}^+$  or  $\text{He}^+$ .

The excited state population is, however, modified by collisions



where X is an electron or proton or possibly a hydrogen atom. These collisions tend to bring the population of the excited states toward thermal equilibrium and thus reduce the intensity of the stimulated radiation.

To date, there have been no measurements of these  $n$ -changing collision processes and all the available information has been obtained theoretically (26). It is evident that this problem is ripe for experimental attack.

Collisions that result in changes in  $l$ ,

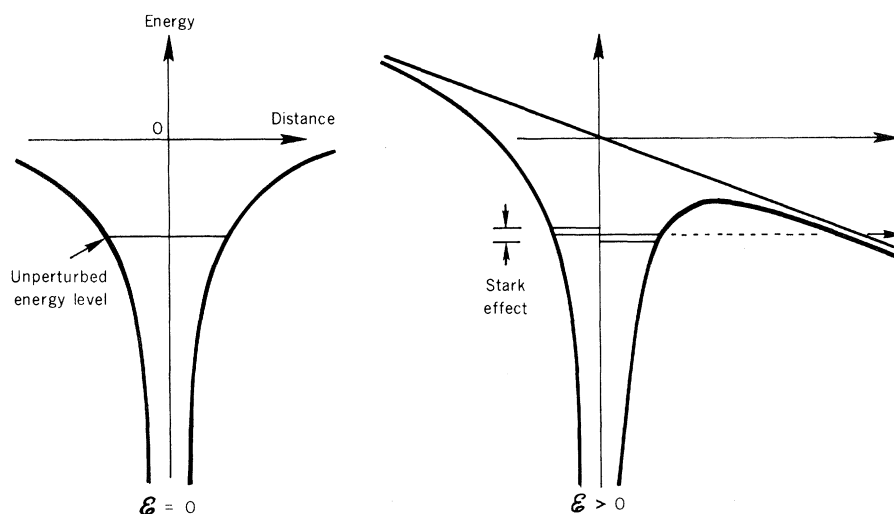


Fig. 5. Potential energy with and without an applied electric field.

however, have apparently been observed by Gallagher *et al.* (27). These authors observed that the fluorescence decay times of sodium atoms in highly excited  $d$  states are lengthened when the atoms collide with rare gas atoms. They interpreted this effect as due to collisional angular momentum mixing of the  $d$  states with states for which  $l > 2$ . At sufficiently high pressures the mixing time is short compared with the radiation lifetime of any of the states. The angular momentum states are thus in equilibrium with one another so that the observed lifetime is the statistically averaged lifetime over all the accessible angular momentum states.

Of great interest also is the collisional ionization process



where  $X$  is again an electron, proton, or hydrogen atom. Experimental techniques are not yet sufficiently advanced that these processes can be studied, although recent developments indicate that their investigation is not far off. In the meantime ionization of highly excited atoms and molecules in collision with various molecules has been studied by a number of groups.

The first measurements of this kind were by Cermak and Herman (4), who created high Rydberg atoms by electron impact with noble gas atoms, and observed the collisional ionization and chemiionization resulting from thermal encounters of these atoms with polyatomic molecules. This work was subsequently extended by others (5-7, 28). Absolute cross sections were obtained for unknown populations of excited states, and the results were in general accord with the calculations of Matsuzawa (29) and Flannery (30).

A significant advance in the study of collisional ionization was made by Chupka (11), who directed light from a highly dispersive vacuum ultraviolet monochromator into a cell containing a mixture of krypton and a target gas. Ions formed in the cell were extracted and their masses were analyzed. The  $Kr^+$  signal resulting from collisions of the type



was determined for a number of well-defined highly excited states.

Related studies have been carried out by West *et al.* (31), who collided a beam of xenon atoms in well-defined highly excited states with  $SF_6$  molecules and detected the resulting positive ions. They obtained absolute cross sections

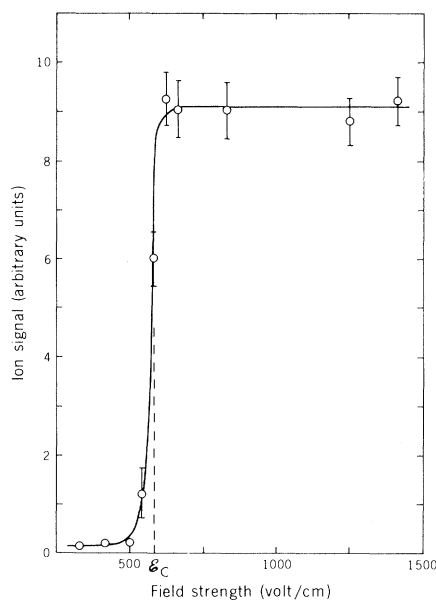


Fig. 6. Ion signal observed as a function of field strength for  $Xe(28f)$ .

for this process for well-defined states  $Xe(nf)$ , with  $25 \leq n \leq 40$ .

These measurements serve a dual purpose. They provide the first absolute data for the process of collisional ionization involving atoms in well-defined highly excited states. In addition, they appear to shed light on the process of low-energy electron scattering. This bonus, which is at first glance surprising, has been discussed at length by Matsuzawa (29) and Flannery (30). They assume, for collisions of the type

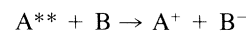


that because of the large radius of the Rydberg orbit, the interaction between the excited electron and the target  $BC$  so greatly exceeds the interaction of the ionic core  $A^+$  with  $BC$  that the latter interaction may be ignored. Thus, apart from its role in transporting the electron into encounters with  $BC$ , the  $A^+$  core acts simply as a spectator to the collision—an inactive but obligatory partner. The electron is assumed to behave as if it were free with an energy which is derived from its orbital motion.

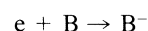
Thus a beam of Rydberg atoms in a collisional ionization experiment may be viewed as equivalent to a beam of electrons whose energy  $E_n$ , comprising both potential energy  $V_n$  and kinetic energy  $T_n$ , is constant. For a Rydberg state with  $l = n - 1$  the classical orbit is circular and the electron velocity is therefore constant with magnitude  $(2|E_n|/m)^{1/2}$ . It thus varies as  $1/n$  and can be incremented in small discrete amounts by changing the quantum state. For a state with  $l < n - 1$  the classical electron orbit is elliptical. Both  $V_n$  and  $T_n$  now vary

with time but the root-mean-square (r.m.s.) electron velocity  $v_1$  is equal to  $(2|E_n|/m)^{1/2}$  and thus varies as  $1/n$  (Table 1). At the present time experimental considerations limit studies of collisional ionization to atoms with  $25 \leq n \leq 40$ , for which the range of electron energies is about 7 to 20 mev. For example, the electron in a  $Xe(28f)$  atom has an r.m.s. energy of about 17 mev.

Developing this model further, Matsuzawa and Flannery show that the rate constant for electron transfer from a high Rydberg atom  $A^{**}$  to molecule  $B$



should be equal to the rate constant for the attachment of free electrons of the same energy to  $B$



Data are available for a preliminary assessment of this prediction for the case of  $SF_6$  (31) and  $CCl_4$  (32) target molecules. For these gases the attachment of free electrons has been studied down to  $\sim 35$  mev ( $SF_6$ ) and  $\sim 55$  mev ( $CCl_4$ ) while the Rydberg measurements provide data up to  $\sim 20$  mev. There is thus no energy overlap between the free electron data and the Rydberg data, and a detailed comparison is therefore not possible. Nonetheless, the data do appear to be in very satisfactory accord. It would be premature to draw any firm conclusions from these results although it seems reasonable to speculate that, in the energy range below  $\sim 25$  mev, conventional techniques with free electrons may, in future, be augmented by studies involving high Rydberg atoms.

#### References

1. A. C. Riviere and D. R. Sweetman, in *Atomic Collision Processes*, M. R. C. McDowell, Ed. (North-Holland, Amsterdam, 1964), pp. 734-742.
2. R. N. Il'in, V. A. Oparin, I. T. Serenkov, E. S. Solov'ev, N. V. Fedorenko, *Sov. Phys. JETP* **32**, 59 (1971).
3. J. E. Bayfield and P. M. Koch, *Phys. Rev. Lett.* **33**, 258 (1974); P. M. Koch and J. E. Bayfield, *ibid.* **34**, 488 (1975).
4. V. Cermak and Z. Herman, *Collect. Czech. Chem. Commun.* **29**, 953 (1964).
5. H. Hotop and A. Niehaus, *J. Chem. Phys.* **47**, 2506 (1967); *Z. Phys.* **215**, 395 (1968).
6. S. E. Kupriyanov, *Sov. Phys. JETP* **21**, 311 (1965); *ibid.* **24**, 674 (1967); *ibid.* **28**, 240 (1969).
7. T. Shibata, T. Fukuyama, K. Kuchitsu, *Chem. Lett.* (1974), p. 75.
8. R. S. Freund, *J. Chem. Phys.* **54**, 3125 (1971); K. C. Smyth, J. A. Schiavone, R. S. Freund, *ibid.* **59**, 5225 (1973); *ibid.* **60**, 1358 (1974).
9. J. A. Schiavone, K. C. Smyth, R. S. Freund, *ibid.* **63**, 1043 (1975).
10. D. E. Donohue, J. A. Schiavone, D. R. Herrick, R. S. Freund, *Bull. Am. Phys. Soc.* **20**, 1458 (1975).
11. W. A. Chupka, *ibid.* **19**, 70 (1974); private communication.
12. F. B. Dunning, F. K. Tittel, R. F. Stebbings, *Opt. Commun.* **7**, 181 (1973).
13. R. F. Stebbings, C. J. Latimer, W. P. West, F. B. Dunning, T. B. Cook, *Phys. Rev. A* **12**, 1453 (1975).
14. T. F. Gallagher, S. A. Edelstein, R. M. Hill, *ibid.* **11**, 1504 (1975); S. Haroche, M. Gross, M. P. Silverman, *Phys. Rev. Lett.* **33**, 1063 (1974).

15. T. W. Ducas, M. G. Littman, R. R. Freeman, D. Kleppner, *Phys. Rev. Lett.* **35**, 366 (1975).
16. M. G. Littman, M. L. Zimmerman, T. W. Ducas, R. R. Freeman, D. Kleppner, *ibid.* **36**, 788 (1976).
17. H. A. Bethe and E. E. Salpeter, *Quantum Mechanics of One and Two Electron Atoms* (Academic Press, New York, 1957).
18. P. M. Koch, L. D. Gardner, J. E. Bayfield, in *Fourth International Conference on Beam Foil Spectroscopy, Gatlinburg, Tenn.* (Plenum, New York, in press).
19. C. Lanczos, *Z. Phys.* **68**, 204 (1931).
20. D. S. Bailey, J. R. Hiskes, A. C. Riviere, *Nucl. Fusion* **5**, 41 (1965).
21. K. B. MacAdam and W. H. Wing, *Phys. Rev. A* **12**, 1464 (1975).
22. S. Svanberg, P. Tsekeris, W. Happer, *Phys. Rev. Lett.* **30**, 817 (1972).
23. C. Fabre, M. Gross, S. Haroche, *Opt. Commun.* **13**, 393 (1975).
24. T. F. Gallagher, R. M. Hill, S. A. Edelstein, *Phys. Rev. Lett.* **35**, 644 (1975).
25. See, for example, I. C. Percival, in *Atoms and Molecules in Astrophysics*, T. R. Carson and M. J. Roberts, Eds. (Academic Press, New York, 1972), pp. 65–83.
26. C. S. Gee, I. C. Percival, J. G. Lodge, D. Richards, in preparation; M. R. Flannery, *J. Phys. B* **8**, 2470 (1975).
27. T. F. Gallagher, S. A. Edelstein, R. M. Hill, *Phys. Rev. Lett.* **35**, 644 (1975).
28. J. A. Stockdale, F. J. Davis, R. N. Compton, C. E. Klots, *J. Chem. Phys.* **60**, 4279 (1974).
29. M. Matsuzawa, *J. Chem. Phys.* **55**, 2685 (1971); *J. Chem. Phys.* **58**, 2674 (1973); *J. Phys. Soc. Jpn.* **32**, 1088 (1972); *ibid.* **33**, 1108 (1972); *J. Electron Spectrosc. Relat. Phenom.* **4**, 1 (1974).
30. M. R. Flannery, *Ann. Phys.* **79**, 480 (1973).
31. W. P. West, G. W. Foltz, F. B. Dunning, C. J. Latimer, R. F. Stebbings, *Phys. Rev. Lett.* **36**, 854 (1976).
32. C. J. Latimer, G. W. Foltz, F. B. Dunning, W. P. West, R. F. Stebbings, in preparation.

## Discovery of Insect Anti-Juvenile Hormones in Plants

Plants yield a potential fourth-generation insecticide.

William S. Bowers, Tomihisa Ohta,  
Jeanne S. Cleere, Patricia A. Marsella

Insect hormones have been researched intensively for about 30 years. Although the genesis of these studies was purely academic, increasing attention has been focused in recent years on the potential use of the insect juvenile hormones (JH) as candidate insecticides.

After some 10 years of research on JH's and active analogs as candidate insecticides, an understanding of their potential efficacy has emerged which indicates some limited practical applications but falls short of the more optimistic predictions expressed in the earlier stages of insect hormone research (1). The main drawback to the usefulness of JH as an insecticide is the short duration of the developmental period during which the insect is sensitive to the application of exogenous JH. The application of excess JH can upset development only during the brief period of metamorphosis that takes place when the immature insect molts to the adult stage; therefore, the application of JH to mixed developmental stages as they occur in most field situations is not sufficiently effective

to provide acceptable insect control. The immature and adult stages are not controlled by excess JH and are able to cause damage such as crop destruction, disease transmission, and the like. Conversely, since JH is necessary throughout most stages of insect life, a hormone antagonist or antihormone would be a more efficacious insecticide. In order to understand the potential utility of such an antihormone, a brief summary of the importance of JH to the growth, development, reproduction, and diapause of insects is necessary.

### Chemistry and Biological Activity of Juvenile Hormone

After the discovery of the JH activity of farnesol (Fig. 1, 1) and farnesal (Fig. 1, 2) by Schmialek (2), Bowers *et al.* (3) obtained a profile of the necessary structural moieties of JH through chemical degradation and regeneration of the JH activity in extracts from cecropia silk moths. This structural information, when incorporated into a sesquiterpenoid framework based on farnesol, resulted in the synthesis of (*E,E*)-10,11-epoxymethylfarnesenate (Fig. 1, 3), which was found to possess all of the

biological activities of the hormone (or hormones) in the cecropia extract. Subsequently, Roller *et al.* (4) isolated and identified a JH from cecropia (Fig. 1, 4) and Meyer *et al.* (5) isolated a second JH from cecropia (Fig. 1, 5). The first hormone (Fig. 1, 3) was later authenticated as a natural hormone from *Manduca* (tobacco hornworm) larval blood (6). After the identification of the natural JH's, many research groups began to study the potential utility of these hormones for insect control. The natural JH's were quickly found to be too labile for field applications, but the discovery of JH activity in certain commercial insecticide synergists (7) revealed the possibility of developing highly active JH analogs containing an aromatic nucleus. Two such aromatic terpenoid ethers (Fig. 1, 6) (8) and (Fig. 1, 7) (9) were developed and are at least a thousand times more active against certain insects than the natural JH's. Zoecon (10) developed a highly active JH analog, Methoprene (Fig. 1, 8), which is now registered for floodwater mosquito control and for the control of flies that breed on manure. It should be made clear that the enthusiasm for developing hormonal methods of insect control is based on the understanding that JH regulates processes in insects for which there are no endocrinological counterparts in man and other so-called higher animals. Adult development in man is dependent on the secretion of certain hormones, especially hypophyseal gonadotropins; conversely, JH's prevent insects from maturing and thus must be absent during the last stages of insect metamorphosis for adult development to occur. When JH is applied to an insect at a time when it should naturally be absent, adult morphogenesis is deranged, resulting in insects with a mosaic of juvenile and adult characters, which are unable to feed, mate, or reproduce and which soon die (11, 12). Although the corpora allata are quiescent during the ultimate stages of metamorphosis, they reawaken in the adult stage and again secrete JH's, which are necessary

Dr. Bowers is an associate professor of entomology, Dr. Ohta is a postdoctoral associate, Ms. Cleere is a research support specialist, and Ms. Marsella is a research technician at the New York State Agricultural Experiment Station, Entomology-Plant Pathology Laboratory, Geneva 14456.